Characterising the effect of large-scale model resolution upon calculated OH production using MOZAIC data

R. A. Crowther,[1] K. S. Law,[1] J. A. Pyle,[1] S. Bekki,[2] and H. G. J. Smit[3]

Received 3 January 2002; revised 20 March 2002; accepted 28 May 2002; published 29 June 2002.

[1] The coarse spatial resolution of large-scale models can be a significant source of error in calculating grid cell averaged rates of physical processes. We investigate here the influence of resolution in the case of chemical reactions. We use high resolution MOZAIC ozone and water vapour data to characterise the effects of unresolved structures on model-calculated production of the hydroxyl radical (OH) in the upper troposphere/lower stratosphere region. The statistical analysis of MOZAIC data indicates that, on average, large-scale models may overestimate OH production by 5% to 20% for resolutions ranging from ~200 to ~800 km respectively. This systematic bias is found to be most significant in the tropopause region. *INDEX TERMS:* 0341 Atmospheric Composition and Structure: Middle atmosphere—constituent transport and chemistry (3334); 0365 Atmospheric Composition and Structure: Troposphere—composition and chemistry; 3210 Mathematical Geophysics: Modeling; 0368 Atmospheric Composition and Structure: Troposphere—constituent transport and chemistry

1. Introduction

[2] There are several possible sources of error in global atmospheric models. For example, those associated with kinetic data (e. g. *Thompson and Stewart* [1991]) or the accuracy of advection schemes (e. g. *Hourdin and Armengaud* [1999]). We focus here on the errors associated with spatial resolution in chemical schemes. Typical spatial resolutions of large-scale chemistry-transport models (CTMs) are 200–500 km horizontal and 1–2 km vertical. Chemistry-climate models are often run at even coarser horizontal resolutions of over 1000 km (e. g. *Pitari and Mancini* [2001]). At present, available computing resources force models to be run at resolutions that can prevent the fine scale structure of the atmosphere being fully resolved. The unresolved spatial variability has some implications for the accuracy of the calculations of the rates of physical processes. Indeed, in the case of processes that depend non-linearly on a spatially variable quantity, the presence of sub-grid scale variability causes a bias between the average of the process rate over the grid cell and the process rate calculated from the grid cell average [*Pincus and Klein*, 2000]. This issue has been extensively investigated in the case of cloud microphysical processes. Cloud schemes in large-scale models attempt to account for some amount of sub-grid scale variability in computing cloud cover, cloud reflectance or rainfall [*Pincus and Klein*, 2000; *Harris and Foufoula-Georgiou*, 2001]. In contrast, little attention has been paid to the resolution issue in the case of chemistry. The possible errors in the calculations of averaged rates of atmospheric chemical processes were first pointed out by *Tuck* [1979] and by *Pyle and Zavody* [1990]. Like most processes in large-scale CTMs, chemical rates are calculated from the values of concentrations averaged over grid cells, ignoring any sub-grid scale variability and correlation between species. There is mounting observational evidence that fine scale structures, often very narrow sheet-like features of less than 1 km in vertical extent, are ubiquitous throughout the troposphere (e. g. *Thouret et al.*, [2000]; *Cho et al.* [2001]). These structures have a wide range of chemical and particulate contents and exhibit steep spatial gradients. The coarse resolution of large-scale models do not allow these structures to be fully resolved. In neglecting small-scale structures and, in a sense, averaging them over relatively large grid cells, there is the potential for significant errors in model-calculated chemical rates.

[3] If one considers a reaction between two chemical species A and B with a rate constant k, which is assumed to be constant for simplification, the instantaneous rate of reaction averaged over a grid cell is [*Pyle and Zavody*, 1990],

$$k\overline{[A][B]} = k\overline{[A]}\ \overline{[B]} + k\overline{[A]'[B]'} \tag{1}$$

with $\overline{[A]'[B]'} = r_{AB}\sigma_A\sigma_B$ where $[A]$ denotes the concentration of the reactant A, $\overline{[A]}$ an average of this concentration over the grid cell, A' a deviation from the average, r_{AB} the linear correlation coefficient between A and B and σ_A the standard deviation of A.

[4] The left-hand term of (1) can be called the true averaged rate. If the concentration fields of reactants A and B within the grid cell are known, the true rate can be obtained by integrating the instantaneous rate over the entire domain of the grid cell. The first term on the right hand side is called the model rate. It is calculated by models from the grid cell averaged values of the A and B concentrations. The second term on the right hand side is the fluctuations covariance term, a measure of the bias in the calculation of the averaged chemical rate when sub-grid variability and correlation in the reactant fields are neglected (i. e. difference between the true rate and the model rate). Note that both sub-grid variability and correlation have to be significant for the occurrence of resolution errors.

[5] The resolution error with respect to the true rate can be expressed as a fractional error

$$\frac{\overline{[A]}\ \overline{[B]} - \overline{[A][B]}}{\overline{[A][B]}} = -\left[1 + \frac{1}{r_{AB}}\frac{\overline{[A]}}{\sigma_A}\frac{\overline{[B]}}{\sigma_B}\right]^{-1} \tag{2}$$

[6] The sign of the resolution error as defined in (2) depends on the correlation between A and B. If the reactants are anti-correlated, the model overestimates the true rate. If they are positively correlated, the model underestimates the rate. The magnitude of the fractional error depends on the correlation and on the relative amount of variability in the reactant fields, namely the standard deviations scaled by the corresponding mean. This fractional variability is obviously resolution-dependent. The higher the model resolution, the smaller the likely variability within the grid cells.

[7] If the rate constant is spatially variable at a sub-grid scale level, the expression (2) can be extended by averaging over the

[1]Centre for Atmospheric Science, Cambridge University, Cambridge, UK.
[2]Service d'Aeronomie du CNRS, Institut Pierre-Simon Laplace, Universite, Paris VI, France.
[3]IGC-2, Forschungszentrum Jülich GmbH, Germany.

0094-8276/02/2002GL014660

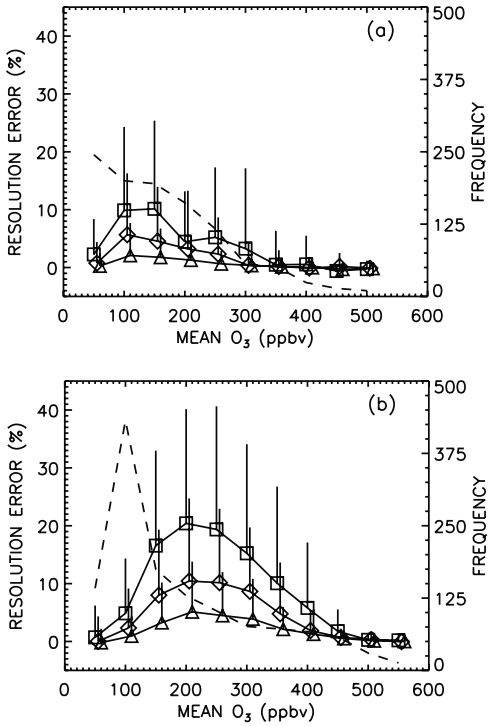

Figure 1. Mean resolution error (%) in $\overline{P(OH)}$ with +1σ deviations as a function of mean O_3 for 15 (triangle), 30 (diamond) and 60 min (square) intervals for (a) winter 97/98 and (b) summer 98. Results are binned according to mean the O_3 value (with each bin covering the mean ±25 ppbv). For statistical significance, only O_3 bins containing at least 5 data records are considered. For clarity, the results for 15 and 30 min intervals are shifted from the central bin value by +10 ppbv and +5 ppbv respectively. Note that H_2O mixing ratios, averaged over the 60 min intervals, range from 5 to 300 ppmv. Also plotted is the number of 60 min intervals per O_3 bin (dashed line).

triple product k[A][B] [*Pyle and Zavody*, 1990]. In the case of self-reaction, the dependency of the rate on the single concentration is quadratic; the bias depends only on the standard deviation and is necessarily positive (models underestimate chemical rates). In the case of a unimolecular reaction, the chemical process is non-linear only if the rate constant is also spatially variable. Note that expression (2) is valid for any physical processes whose rates can be expressed as a product of variable quantities.

[8] The purpose of this work is to provide a preliminary estimate of the effects of finite spatial resolution with specific attention to the important upper troposphere and lower stratosphere (UT/LS) region. Most of the climate sensitivity in this region originates from ozone and water vapour, particularly around the tropopause where steep spatial gradients prevail. O_3 and H_2O are also the main precursors for the highly reactive hydroxyl radical, OH. OH is a key species in potential chemistry-climate feedbacks because it is the primary oxidant for most source gases in the atmosphere and, hence, determines the global oxidising capacity of the atmosphere. O_3 and H_2O have been measured on a regular basis aboard commercial aircraft within the framework of the EU-funded MOZAIC (Measurement of OZone and water vapour by Airbus In-service airCraft) project [*Marenco et al.*, 1998]. These high-resolution quality-controlled O_3 and H_2O data represent an excellent opportunity to characterise sub-grid scale structures and correlations in O_3 and H_2O fields around the tropopause and to investigate the implications for the OH production calculated in large-scale models. Details about the instrumentation and the quality of the data can be found in the literature [*Marenco et al.*, 1998; *Thouret et al.*, 1998; *Helten et al.*, 1999].

2. Data analysis

[9] An assumption is made that the primary production of OH in the tropopause region, P(OH), can be expressed approximately as,

$$P(OH) = \frac{2k_1 J_{O_3}}{(k_2[O_2] + k_3[N_2])}[O_3][H_2O] \quad (3)$$

where J_{O_3} is photolysis rate of O_3 to produce $O(^1D)$ and k_1, k_2 and k_3 are the rate constants for the reactions between $O(^1D)$ with H_2O, O_2 and N_2 respectively. This assumption is supported in part by the results of *Jaeglé et al.*, [2000], who concluded that the primary sources of HO_x in the North Atlantic tropopause region were principally $O(^1D) + H_2O$ and acetone photolysis.

[10] To a first order, P(OH), as defined in (3), can be assumed to be proportional to the product of $[O_3]\times[H_2O]$. Indeed, the rate constants involved in (3) have no temperature dependency (for k_1) or a weak temperature dependency (for k_2 and k_3) and should, therefore, vary little over a large grid cell, even in the presence of strong temperature gradients. Furthermore, the local variations in the concentrations of O_2 and N_2 should be small because aircraft tend to fly on constant pressure levels at cruise altitude. Finally, the photolysis rate of O_3 can vary very strongly over a large grid cell, especially at high zenith angles. However, there is no reason to expect any significant correlation between J_{O_3} and the local concentration of long-lived tracers such as O_3 and H_2O in the UT/LS region.

[11] The MOZAIC measurements of O_3 and H_2O are made every 4 seconds. Only data taken at cruise altitude within the North Atlantic flight corridor are considered because this is the most intensively scanned region by MOZAIC commercial aircraft and, hence, leads to the most statistically significant results. A total of 216 flights made during winter 1997/1998 (December, January, February) and 232 flights from summer 1998 (June, July, August) have been analysed. The data analysis performed here is similar to the one described in *Sparling et al.*, [1998].

[12] The true averaged rate as defined in (2) is calculated from the high-resolution data. The resolution errors are derived from means, standard deviations and correlation coefficient of O_3 and H_2O over time intervals of 15, 30 to 60 mins which are approximately equivalent to length intervals of 200, 400 and 800 km assuming a cruise speed of around 800 km hr^{-1}. Intervals containing less than ten records are discarded. The intensive averaging tends to ensure that random data errors have a marginal effect on the calculations of means, although they would increase the standard deviations but decrease the correlations. In addition, any "scaling" errors in the data would not affect the results regarding the relative errors.

3. Results

[13] Figure 1 shows the mean percentage resolution error in $\overline{P(OH)}$ calculated at different averaging time intervals (15, 30 and 60 minutes) for winter and summer. The percentage resolution error is calculated from the statistical quantities on the right-hand side of expression (2). As expected, this gives the same errors as those calculated from the left-hand side of expression (2), i. e. the mean difference between $\overline{P(OH)}$ calculated using the original 4 sec data and $\overline{P(OH)}$ calculated from averaged data. The $\overline{P(OH)}$ data are binned according to their mean O_3 mixing ratios, with a minimum of five values per bin. The data are all taken well within the UT/LS region (MOZAIC aircraft generally cruise at altitudes of between 9 and 13 km). For data averaged over 15 minutes, which

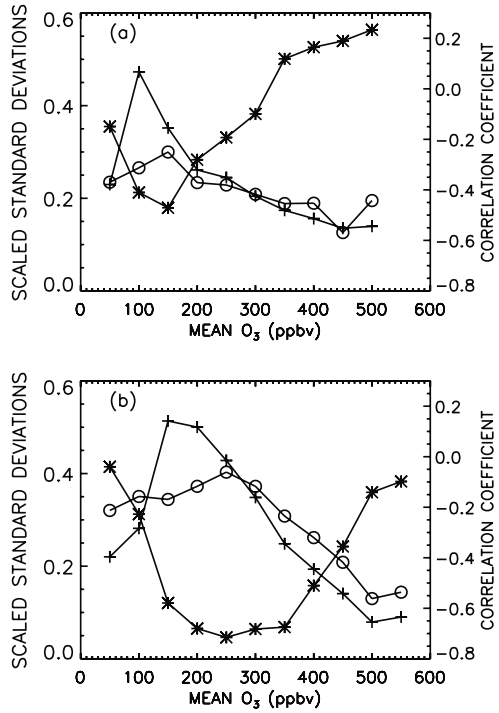

Figure 2. The mean scaled standard deviations of O_3 (cross) and H_2O (circle) (scaled by the corresponding mean value) and the linear correlation coefficient (asterisk, plotted on the secondary y-axis) as a function of the mean O_3 value for an averaging time interval of 60 min for (a) winter 97/98 and (b) summer 98. The same O_3 bins have been used as in Figure 1.

is equivalent to 200 km resolution, there is a systematic difference between low and high resolution $\overline{P(OH)}$ of up to +2% in winter and up to +5% in summer. This implies that large-scale models overestimate the true $\overline{P(OH)}$. As the resolution is degraded to about 400 km (30 minutes), the maximum systematic bias increases to 6% in winter and 11% in summer. This is a common CTM resolution (between T21 and T42 in the mid-latitudes) and so one could expect a typical CTM to overestimate $\overline{P(OH)}$ by up to 11% in the summer months. At even coarser resolution (~800 km), the systematic bias peaks at 10% in winter and 20% in summer. This low resolution is more common for multi-annual CTM simulations. The $+1\sigma$ deviations are also shown on Figure 1, suggesting that models could overestimate $\overline{P(OH)}$ by more than 40% in some cases.

[14] Errors are very small for O_3 mixing ratios less than 50 ppbv and greater than 300 ppbv in the winter and less than 50 ppbv and greater than 450 ppbv in the summer. The errors tend to peak at O_3 values of 100 to 150 ppbv in the winter and between 200 and 250 ppbv in the summer. The 100–450 ppbv range corresponds to the few kilometers thick transition region encompassing the tropopause. It is characterised by very sharp gradients in ozone, usually a jump from 60–80 ppbv to few hundreds of ppbv, and in water vapour. *Gierens et al.* [1999] identified the tropopause with an ozone mixing ratio of 130 ppbv. They stressed that this threshold value is a mean ozone concentration at the thermal tropopause with a large standard deviation of 92 ppbv. A large part of this deviation must originate from seasonal variations. An analysis of Canadian ozonesonde data by *Logan* [1999] indicates that median values of ozone at the thermal tropopause vary typically from about 70 ppbv in the winter to 150 ppbv in the summer with O_3 values being 50–100% lower 1 km below the tropopause and about a factor 2–3 higher 2 km above the tropopause. The resolution error appears to be most significant in the tropopause region with a pattern which tends to follow the tropopause.

[15] Figure 2 shows the standard deviations of O_3 and H_2O, scaled by the means, along with the linear correlation coefficient as a function of the mean O_3 for an averaging time interval of 60 minutes for winter and summer. This figure indicates which terms in the right-hand side of (2) contribute most to the errors. The correlation coefficient and the O_3 sub-grid variability are found to be the most important factors. Their variations with mean O_3 are very similar. The correlation peaks at −0.5 at ~150 ppbv of O_3 in winter and at −0.7 at 200 ppbv in summer. This strong anti-correlation originates from the mixing of tropospheric (high H_2O, low O_3) and stratospheric (low H_2O, high O_3) air masses in the tropopause region. The mean-scaled O_3 standard deviation peaks at almost 0.5 at ~100 ppbv of O_3 in winter. In summer the standard deviation is similar, but at a higher O_3 mixing ratio of 150 ppbv. The correlation and the O_3 sub-grid variability drop rapidly outside the tropopause region. This pattern matches well the variations in the resolution errors (see Figure 1). The H_2O sub-grid variability exhibits a similar pattern to the O_3. The highest values of scaled H_2O standard deviation are found in the tropopause region. However, the values are not quite as large as those for O_3, peaking at 0.3 and 0.4 in winter and summer respectively. Also, these peak values occur at higher mean O_3 values.

4. Discussion

[16] We have shown that model resolution errors could be particularly important in the calculation of primary OH production in the tropopause region. However, there are possible uncertainties associated with our results which need to be recognised. It is not clear to what extent one-dimensional MOZAIC transects over the North Atlantic are representative of the whole UT/LS region. For instance, any bias in the temporal and spatial data sampling such as the relatively high weight given to the jet stream zone in the MOZAIC dataset [*Gierens et al.*, 1999], might lead to bias in estimating the spatially integrated resolution effect for the whole UT/LS region [*Sparling et al.*, 1998]. We have not calculated the full impact of averaging errors on OH, or other species in the UT/LS, as this would require a full photochemical model calculation. The overestimation of the primary OH production rate could be mitigated, or amplified, by other erroneously calculated averaged chemical rates. Indeed, a large number of other key chemical species such as NO_y (sum of all oxidised nitrogen species except N_2O) or CO also exhibit steep gradients across the tropopause region with some degree of spatial correlation between them [*Fischer et al.*, 2000]. In addition, the analysis of errors in the OH production is, in reality, more complex. Since photolysis followed by reaction with water vapour is one of the main chemical sinks for O_3, OH and O_3 are intimately coupled and, hence, any errors in OH will affect O_3.

[17] Large-scale models are our main tools in deriving global O_3 and HO_x budgets and in investigating chemistry-climate feedbacks, particularly those associated with the UT/LS region. We have identified a systematic bias associated with sub-grid scale variability which may require corrections to be applied to global models. Subgrid scale variability is currently taken into account to some extent in convection and advection schemes. The sub-grid distribution assumed in these schemes could be used within model chemistry schemes to calculate chemical rates averaged over grid cells (e. g. *Chipperfield* [1999]).

[18] **Acknowledgments.** This work has been supported by the Environment and Climate Research Programme of the European Commission under the on-going contracts No. EVK2-1999-00141 (MOZAIC III) and No. EVK2-CT-2001-00112 (PARTS). This work was also supported by the NERC funded U. K. Universities Global Atmospheric Modelling Programme. We also acknowledge J.-P. Cammas (Laboratoire d'Aerologie) for provision of the MOZAIC O_3 data. We thank Air France, Lufthansa,

Austrian Airlines, and Sabena for carrying the MOZAIC equipment free of charge and for performing maintenance.

References

Chipperfield, M. P., The effects of sub-gridscale features on stratospheric chemistry in large-scale models, *Mesoscale Processes in the Stratosphere*, Air Pollution Research Report no. 69, European Commission, 41–46, 1999.

Cho, J. Y. N., R. E. Newell, and E. V. Browell, et al., Observation of pollution plume capping by a tropopause fold, *Geophys. Res. Lett.*, *28*, 3243–3246, 2001.

Fischer, H., F. G. Wienhold, and P. Hoor, et al., Tracer correlations in the northern high latitude lowermost stratosphere: Influence of cross-tropopause mass exchange, *Geophys. Res. Lett.*, *27*, 97–100, 2000.

Gierens, K., U. Schumann, M. Helten, H. Smit, and A. Marenco, A distribution law for relative humidity in the upper troposphere and lower stratosphere derived from three years of MOZAIC measurements, *Ann. Geophysicae*, *17*, 1218–1226, 1999.

Helten, M., H. G. J. Smit, D. Kley, et al., In-flight comparison of MOZAIC and POLINAT water vapor measurements, *J. Geophys. Res.*, *104*, 26,087–26,096, 1999.

Hourdin, F., and A. Armengaud, The use of finite-volume methods for atmospheric advection of trace species. Part I: Test of various formulations in a general circulation model, *Mon. Weather Rev.*, *127*, 822–837, 1999.

Jaeglé, L., D. J. Jacob, W. H. Brune, et al., Photochemistry of HO_x in the upper troposphere at northern midlatitudes, *J. Geophys. Res.*, *105*, 3877–3892, 2000.

Logan, J. A., An analysis of ozonesonde data for the troposphere: Recommendations for testing three-dimensional models and development of a gridded climatology for tropospheric ozone, *J. Geophys. Res.*, *104*, 16,115–16,141, 1999.

Marenco, A., V. Thoruret, P. Nedelec, et al., Measurement of ozone and water vapor by Airbus in-service aircraft: The MOZAIC airborne program, An overview, *J. Geophys. Res.*, *103*, 25,631–25,642, 1998.

Pincus, R., and S. A. Klein, Unresolved spatial variability and microphysical process rates in large-scale models, *J. Geophys. Res.*, *105*, 27,059–27,065, 2000.

Pitari, G., and E. Mancini, Climatic impact of future supersonic aircraft: Role of water vapour and ozone feedback on circulation, *Phys. Chem. Earth Part C*, *26*, 571–576, 2001.

Pyle, J. A., and A. M. Zavody, The modelling problems associated with spatial averaging, *Q. J. R. Meteorol. Soc.*, *116*, 753–766, 1990.

Sparling, L. C., A. R. Douglass, and M. R. Schoeberl, An estimate of the effect of unresolved structure on modeled ozone loss from aircraft observations of ClO, *Geophys. Res. Lett.*, *25*, 305–308, 1998.

Thompson, A. M., and R. W. Stewart, Effect of chemical-kinetics uncertainties on calculated constituents in a tropospheric photochemical model, *J. Geophys. Res.*, *96*, 13,089–13,108, 1991.

Thouret, V., A. Marenco, J. A. Logan, P. Nedelec, and C. Grouhel, Comparisons of ozone measurements from the MOZAIC airborne program and the ozone sounding network at eight locations, *J. Geophys. Res.*, *103*, 25,695–25,720, 1998.

Thouret, V., J. Y. N. Cho, R. E. Newell, A. Marenco, and H. Smit, General characteristics of tropospheric trace constituent layers observed in the MOZAIC program, *J. Geophys. Res.*, *105*, 17,379–17,392, 2000.

Tuck, A. F., A comparison of one-, two-, and three-dimensional model representations of stratospheric gases, *Philos. Trans. R. Soc. London, Ser. A*, *290*, 477–494, 1979.

R. A. Crowther, K. S. Law, and J. A. Pyle, Centre for Atmospheric Science, Cambridge University, Chemistry Department, Lensfield Road, Cambridge CB2 1EW, UK. (richard.crowther@atm.ch.cam.ac.uk)

S. Bekki, Service d'Aeronomie du CNRS, Institut Pierre-Simon Laplace, Universite Paris VI, Paris, France. (Slimane.Bekki@aero.jussieu.fr)

H. G. J. Smit, IGC-2, Forschungszentrum Jülich GmbH, D-52425 Jülich, Germany. (h.smit@fz-juelich.de)